**Far East Journal of Mathematical Sciences (FJMS)**

http://www.pphmj.com
http://dx.doi.org/10.17654/MS131010069
Volume 131, Number 1, 2021, Pages 69-82 **ISSN: 0972-0871**

# STOCHASTIC NONLINEAR DYNAMICS OF ERYTHROCYTE DEFORMATION: APPLICATION TO DEOXY-HEMOGLOBIN S

**S. Massou, O. W. Akadry and A. L. Essoun**

Department of Physics
Faculty of Science and Technology
University of Abomey-Calavi
06 BP: 1716 Cotonou
Republic of Benin
e-mail: siakmas@yahoo.fr
wadoudiakadry@gmail.com

## Abstract

We present a study of the nonlinear effects generated by Gaussian noise on the dielectric permittivity of deoxy-hemoglobin S. In this work, we have developed new theories of the dielectric permittivity of deoxy-hemoglobin S. We have shown that, only a fine analysis of the spectral curve makes it possible to obtain sufficient precision to describe the phenomenon of frequency deformation of erythrocytes. We have found that the theories developed are stable methods up to 2% of Gaussian noise. We have detected parameters allowing to calculate the hematocrit level $\left(Q = \frac{\omega_0}{\Delta\omega}\right)$ from relaxation spectra to explain chronic hemolytic anemia caused by dehydration in sickle cell patients.

Received: May 6, 2021; Accepted: June 9, 2021

2020 Mathematics Subject Classification: 92C37.

Keywords and phrases: dielectric permittivity, deoxy-hemoglobin S, chronic hemolytic anemia.

## 1. Introduction

The transformation of hemoglobin S gel solution was first described by Hofrichter et al. [3] and Harris and Bensusan [2]. The main problem that still arises revolves around the relationship between dielectric spectra and the microscopic hemoglobin's properties in blood. This description is complicated and so far there is no generally accepted approach to the problem posed. The objective of this article is to address the nonlinearity of the dielectric permittivity of hemoglobin S gel solution in the presence of Gaussian noise. We show that the nonlinear effects arise from the presence of Gaussian white noise. The aim of our study was therefore to understand the molecular mechanism of erythrocyte deformation kinetics from nonlinear theoretical models of dielectric permittivity in order to extract information from the characteristic parameters of the dielectric to limit the dehydration of hemoglobin S.

## 2. Material and Methods

The developed mathematical theory [6] is a good model of interpretation. After adequate approximations, we have defined the dielectric dispersion function which has the same analytical form as that obtained in the previous work [6] to describe the structural viscosity of the solution-gel of hemoglobin S. Nonlinear theoretical formula of the complex dielectric permittivity has the analytical form defined by:

$$\frac{\varepsilon^*(\tau, \omega)}{\varepsilon_\infty} = \left[1 - (1 - \chi)\frac{1}{1 + j\omega\tau}\right]^{-\nu}. \tag{1.1}$$

We can write:

$$\frac{\varepsilon^*(\tau, \omega)}{\varepsilon_\infty} = \left[1 - (1 - \chi)\frac{1 - j\omega\tau}{1 + \omega^2\tau^2}\right]^{-\nu} \tag{1.2}$$

with

$$\chi = \left(\frac{\varepsilon_\infty}{\varepsilon_0}\right)^{1/\nu}, \tag{1.3}$$

where $j^2 = -1$; the relaxation frequency $(\omega)$ is the controlling factor; $(\tau)$ is the relaxation or delay time and the parameter $(\nu)$ is a real physical parameter which represents the percentage of Gaussian noise.

Let us pose:

$$\eta = \frac{1-\chi}{1+\omega^2\tau^2}. \tag{1.4}$$

By transforming the relation (1.2), we obtain:

$$\frac{\varepsilon^*(\tau,\ \omega)}{\varepsilon_\infty} = [1-\eta(1-\ j\omega\tau)]^{-\nu} = [(1-\eta)+\eta j\omega\tau]^{-\nu}. \tag{1.5}$$

Relation (1.5) can still be written as:

$$\frac{\varepsilon^*(\tau,\ \omega)}{\varepsilon_\infty} = [\xi\exp(j\theta)]^{-\nu} = \frac{\exp(-j\nu\theta)}{\xi^\nu}. \tag{1.6}$$

The modulus and the argument are given, respectively, by the following expressions (1.7) and (1.8):

$$\xi = [(1-\eta)^2 + \eta^2\omega^2\tau^2]^{\frac{1}{2}}, \tag{1.7}$$

$$\theta = \arctan\left(\frac{\eta\omega\tau}{1-\eta}\right). \tag{1.8}$$

The dielectric dispersion function becomes:

$$\varepsilon^*(\tau,\ \omega) = \frac{\varepsilon_\infty}{\xi^\nu}[\cos(\nu\theta) - j\sin(\nu\theta)]. \tag{1.9}$$

The real part of the complex quantity (1.9) represents the real permittivity of the dielectric, its expression is given by the relation (1.10):

$$\varepsilon'(\tau,\ \omega) = \frac{\varepsilon_\infty}{\xi^\nu}\cos(\nu\theta). \tag{1.10}$$

The imaginary part of the complex quantity (1.9) represents the intrinsic power dissipation of the dielectric, given by the relation (1.11):

$$\varepsilon''(\tau, \omega) = \frac{\varepsilon_\infty}{\xi^\nu} \sin(\nu\theta). \tag{1.11}$$

By suitable transformations of relations (1.10) and (1.11), we obtain general expressions of the real permittivity and the intrinsic power dissipation as a function of the characteristic parameters $(\varepsilon_0; \varepsilon_\infty; \tau; \nu)$.

For $2\kappa \leq \nu$:

The real permittivity is given by the relation:

$$\varepsilon'(\tau, \omega) = \varepsilon_\infty \sum_{\kappa=0}^{\nu} \frac{(-1)^\kappa C_\nu^{\nu-2\kappa} (1 + \omega^2\tau^2 - \gamma)^{\nu-2\kappa} (\gamma\omega\tau)^{2\kappa}}{(1 + \omega^2\tau^2 - 2\gamma + \gamma^2)^\nu}. \tag{1.12}$$

For $2\kappa + 1 \leq \nu$:

Intrinsic power dissipation takes the form of:

$$\varepsilon''(\tau, \omega) = \varepsilon_\infty \sum_{\kappa=0}^{\nu} \frac{(-1)^\kappa C_\nu^{\nu-2\kappa-1} (1 + \omega^2\tau^2 - \gamma)^{\nu-2\kappa-1} (\gamma\omega\tau)^{2\kappa+1}}{(1 + \omega^2\tau^2 - 2\gamma + \gamma^2)^\nu} \tag{1.13}$$

with

$$\gamma = 1 - \chi. \tag{1.14}$$

Recall that the parameter $(\nu)$ is the positive real parameter defined upper, with $(\nu \geq 1)$.

For $\nu = 1$:

$$\varepsilon'(\tau, \omega) = \varepsilon_\infty \frac{1 + \omega^2\tau^2 - \gamma}{1 + \omega^2\tau^2 - 2\gamma + \gamma^2}, \tag{1.15}$$

$$\varepsilon''(\tau, \omega) = \varepsilon_\infty \frac{\gamma\omega\tau}{1 + \omega^2\tau^2 - 2\gamma + \gamma^2}. \tag{1.16}$$

For $\nu = 2$:

$$\varepsilon'(\tau, \omega) = \varepsilon_\infty \frac{(1 + \omega^2\tau^2 - \gamma)^2 - (\gamma\omega\tau)^2}{(1 + \omega^2\tau^2 - 2\gamma + \gamma^2)^2}, \tag{1.17}$$

$$\varepsilon''(\tau, \omega) = \varepsilon_\infty \frac{2(1 + \omega^2\tau^2 - \gamma)(\gamma\omega\tau)}{(1 + \omega^2\tau^2 - 2\gamma + \gamma^2)^2}. \tag{1.18}$$

For $\nu = 3$:

$$\varepsilon'(\tau, \omega) = \varepsilon_\infty \frac{(1 + \omega^2\tau^2 - \gamma)^3 - 3(1 + \omega^2\tau^2 - \gamma)(\gamma\omega\tau)^2}{(1 + \omega^2\tau^2 - 2\gamma + \gamma^2)^3}, \tag{1.19}$$

$$\varepsilon''(\tau, \omega) = \varepsilon_\infty \frac{-(\gamma\omega\tau)^3 + 3(1 + \omega^2\tau^2 - \gamma)^2(\gamma\omega\tau)}{(1 + \omega^2\tau^2 - 2\gamma + \gamma^2)^3}. \tag{1.20}$$

## 3. Results and Discussion

### 3.1. Dielectric permittivities of four samples of deoxy-hemoglobin S

#### 3.1.1. Solution 1 ($\varepsilon_0 = 114$; $\varepsilon_\infty = 56$)

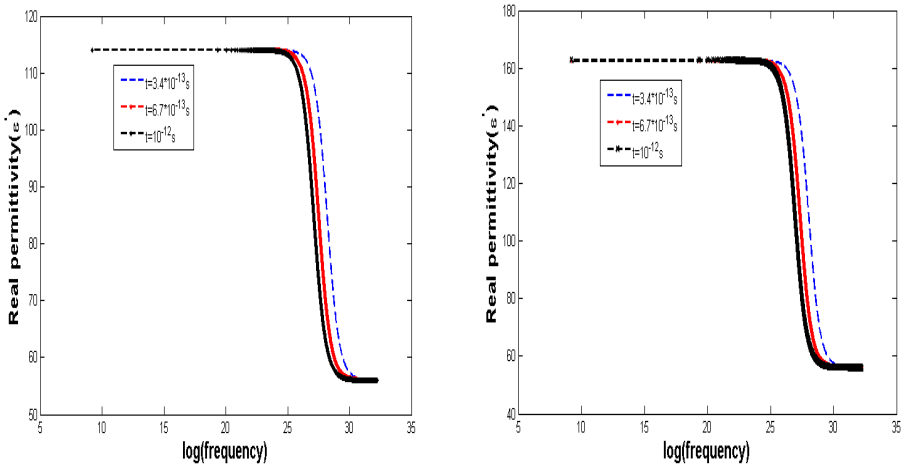


(a) (b)

**Figure 1.1.** Evolution of real permittivity at 2% (a) and 3% (b) of the Gaussian noise.

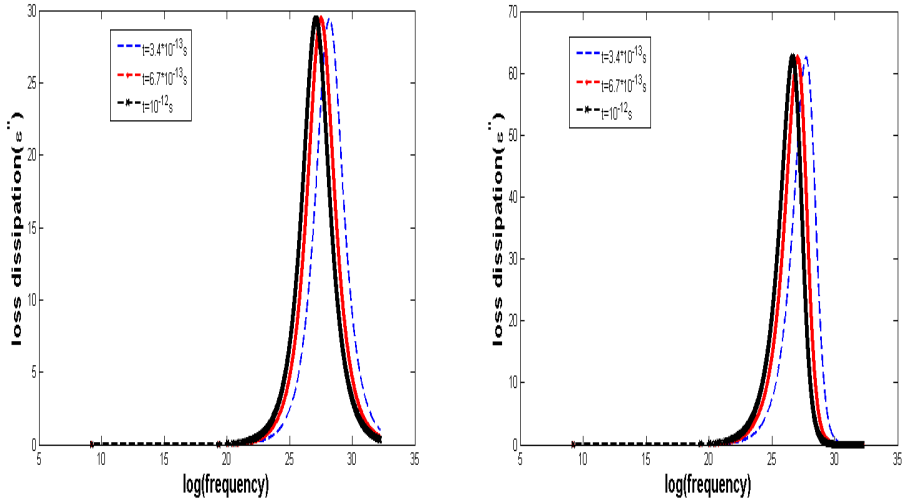


**Figure 1.2.** Evolution of intrinsic power dissipation of deoxy-hemoglobin S at 2% (a) and 3% (b) of Gaussian noise.

**Table 1.** At 2% of Gaussian noise

| Time to relaxation $\tau$ | Power at resonance | Frequency at resonance | Frequency bandwidth | Rate hematocrit |
|---|---|---|---|---|
| $3.4 * 10^{-13}$s | 29.4325 | $1.7430 * 10^{12}$Hz | $3.3732 * 10^{12}$Hz | 51.67% |
| $6.7 * 10^{-13}$s | 29.4325 | $8.8450 * 10^{11}$Hz | $17.12 * 10^{11}$Hz | 51.66% |
| $10^{-12}$s | 29.4325 | $5.9275 * 10^{11}$Hz | $11.47 * 10^{11}$Hz | 51.67% |

**Table 2.** At 3% of Gaussian noise

| Time to relaxation | Power at resonance | Frequency at resonance | Frequency bandwidth | Rate hematocrit |
|---|---|---|---|---|
| $3.4 * 10^{-13}$s | 62.5519 | $1.0960 * 10^{12}$Hz | $1.5423 * 10^{12}$Hz | 71.06% |
| $6.7 * 10^{-13}$s | 62.5519 | $5.5625 * 10^{11}$Hz | $7.827 * 10^{11}$Hz | 71.06% |
| $10^{-12}$s | 62.5519 | $3.7275 * 10^{11}$Hz | $5.245 * 10^{11}$Hz | 71.06% |

**3.1.2. Solution 2** ($\varepsilon_0 = 104$; $\varepsilon_\infty = 54$)

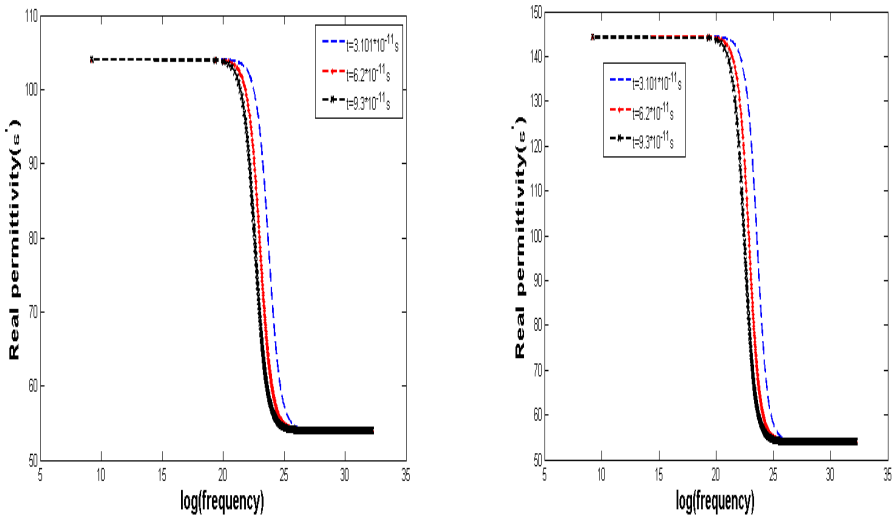


(a) (b)

**Figure 1.3.** Evolution of real permittivity at 2% (a) and 3% (b) of the Gaussian noise.

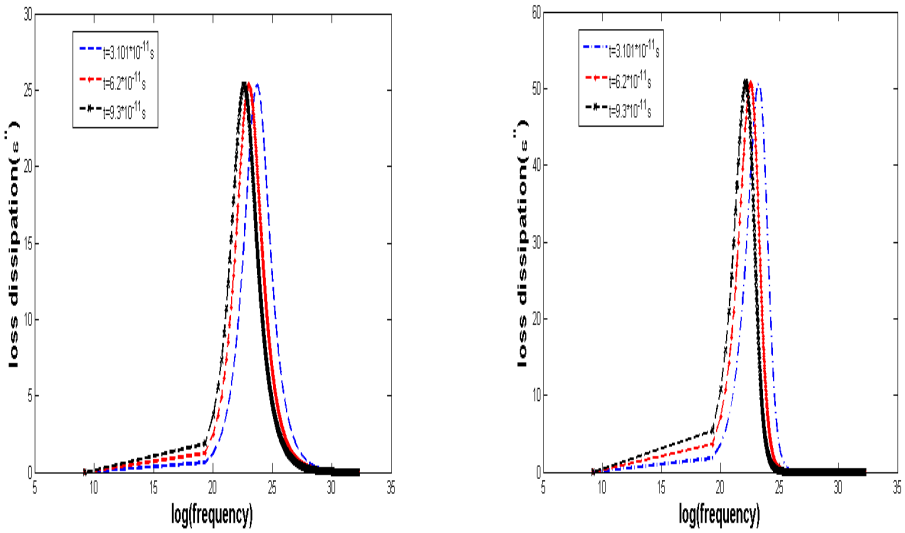


(a) (b)

**Figure 1.4.** Evolution of intrinsic power dissipation of deoxy-hemoglobin S at 2% (a) and 3% (b) of Gaussian noise.

**Table 3.** At 2% of Gaussian noise

| Time to relaxation | Power at resonance | Frequency at resonance | Frequency bandwidth | Rate hematocrit |
|---|---|---|---|---|
| $3.101 * 10^{-11}$s | 25.3191 | $2 * 10^{10}$Hz | $3.9 * 10^{10}$Hz | 51.28% |
| $6.2 * 10^{-11}$s | 25.3191 | $1 * 10^{10}$Hz | $1.975 * 10^{10}$Hz | 50.63% |
| $9.3 * 10^{-11}$s | 25.3153 | $6.75 * 10^{9}$Hz | $13 * 10^{9}$Hz | 51.92% |

**Table 4.** At 3% of Gaussian noise

| Time to relaxation | Power at resonance | Frequency at resonance | Frequency bandwidth | Rate hematocrit |
|---|---|---|---|---|
| $3.101 * 10^{-11}$s | 50.6930 | $1.25 * 10^{10}$Hz | $1.775 * 10^{10}$Hz | 70.42% |
| $6.2 * 10^{-11}$s | 50.6930 | $6.25 * 10^{9}$Hz | $9 * 10^{9}$Hz | 69.44% |
| $9.3 * 10^{-11}$s | 50.6693 | $4.25 * 10^{9}$Hz | $6 * 10^{9}$Hz | 70.83% |

### 3.1.3. Solution 3 ($\varepsilon_0 = 99$; $\varepsilon_\infty = 52$)

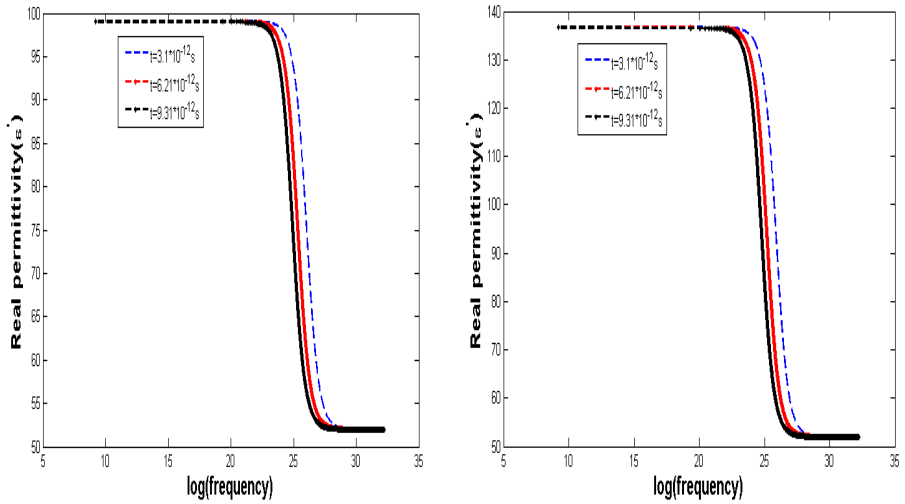


(a) (b)

**Figure 1.5.** Evolution of real permittivity at 2% (a) and 3% (b) of the Gaussian noise.

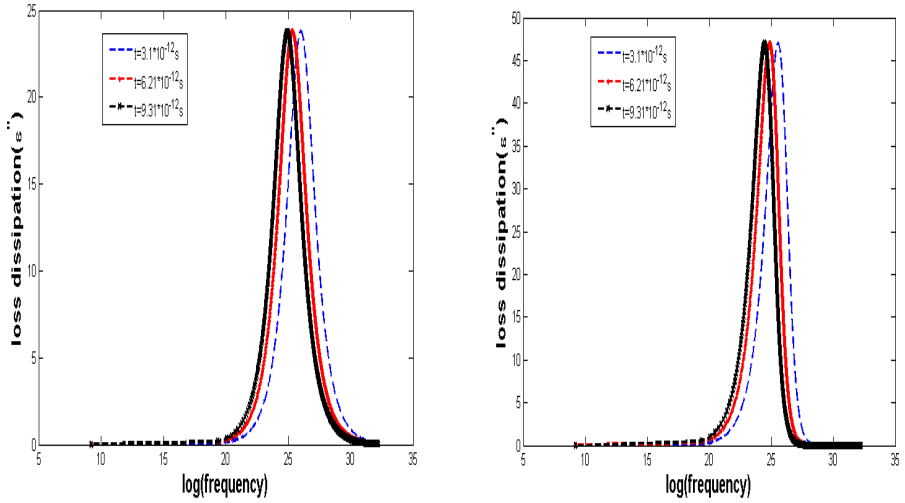


**Figure 1.6.** Evolution of intrinsic power dissipation of deoxy-hemoglobin S at 2% (a) and 3% (b) of Gaussian noise.

**Table 5.** At 2% of Gaussian noise

| Time to relaxation | Power at resonance | Frequency at resonance | Frequency bandwidth | Rate hematocrit |
|---|---|---|---|---|
| $3.11 * 10^{-12}$s | 23.7903 | $2 * 10^{11}$Hz | $3.8925 * 10^{11}$Hz | 51.38% |
| $6.21 * 10^{-12}$s | 23.7903 | $10^{11}$Hz | $1.95 * 10^{11}$Hz | 51.28% |
| $9.31 * 10^{-12}$s | 23.7903 | $6.6750 * 10^{10}$Hz | $13 * 10^{10}$Hz | 51.34% |

**Table 6.** At 3% of Gaussian noise

| Time to relaxation | Power at resonance | Frequency at resonance | Frequency bandwidth | Rate hematocrit |
|---|---|---|---|---|
| $3.11 * 10^{-12}$s | 47.0443 | $1.2475 * 10^{11}$Hz | $1.76 * 10^{11}$Hz | 70.88% |
| $6.21 * 10^{-12}$s | 47.0443 | $6.25 * 10^{10}$Hz | $8.85 * 10^{10}$Hz | 70.62% |
| $9.31 * 10^{-12}$s | 47.0442 | $4.1750 * 10^{10}$Hz | $5.9 * 10^{10}$Hz | 70.76% |

### 3.1.4. Solution 4 ($\varepsilon_0 = 92$; $\varepsilon_\infty = 47$)

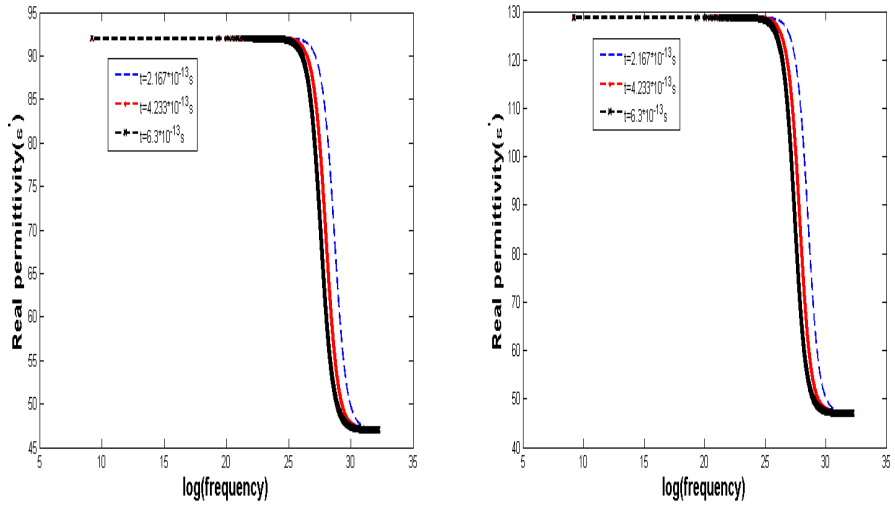


(a) (b)

**Figure 1.7.** Evolution of real permittivity at 2% (a) and 3% (b) of the Gaussian noise.

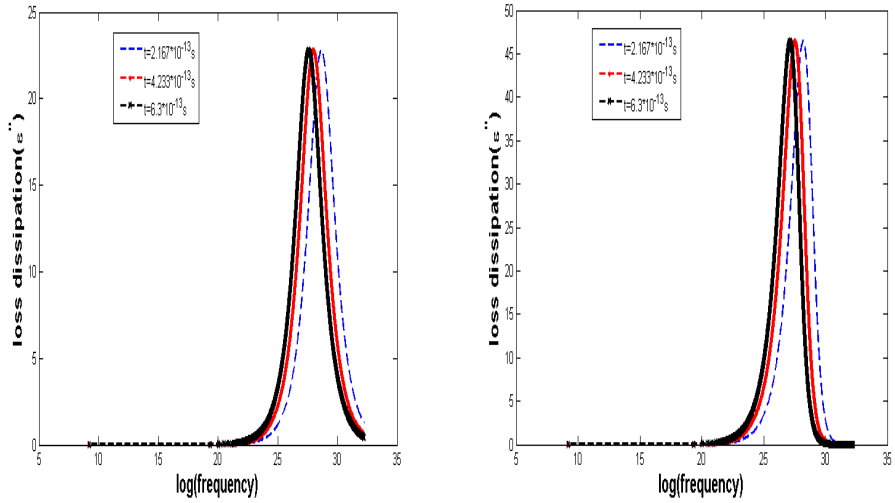


(a) (b)

**Figure 1.8.** Evolution of intrinsic power dissipation of deoxy-hemoglobin S at 2% (a) and 3% (b) of Gaussian noise.

**Table 7.** At 2% of Gaussian noise

| Time to relaxation | Power at resonance | Frequency at resonance | Frequency bandwidth | Rate hematocrit |
|---|---|---|---|---|
| $2.167 * 10^{-13}$s | 22.8013 | $2.8128 * 10^{12}$Hz | $5.4617 * 10^{12}$Hz | 51.50% |
| $4.233 * 10^{-13}$s | 22.8013 | $1.4398 * 10^{12}$Hz | $2.7955 * 10^{12}$Hz | 51.50% |
| $6.3 * 10^{-13}$s | 22.8013 | $9.6750 * 10^{11}$Hz | $18.787 * 10^{11}$Hz | 51.49% |

**Table 8.** At 3% of Gaussian noise

| Time to relaxation | Power at resonance | Frequency at resonance | Frequency bandwidth | Rate hematocrit |
|---|---|---|---|---|
| $2.167 * 10^{-13}$s | 46.4577 | $1.7613 * 10^{12}$Hz | $2.48 * 10^{12}$Hz | 71.02% |
| $4.233 * 10^{-13}$s | 46.4577 | $9.0150 * 10^{12}$Hz | $12.692 * 10^{12}$Hz | 71.02% |
| $6.3 * 10^{-13}$s | 46.4577 | $6.0575 * 10^{11}$Hz | $8.53 * 10^{11}$Hz | 71.01% |

### 3.2. Analysis and validity of the nonlinear dynamic model

It is interesting to observe that the theoretical spectra of the real permittivity and the intrinsic power dissipation qualitatively reproduce the essential characteristics of the relaxation curves. The intrinsic power dissipation spectra are varied depending on the relaxation time. The power at resonance increases with increasing Gaussian noise. The intrinsic power dissipation curves obtained at 1% and at 2% of Gaussian noise are almost the same. The curves are spaced and the intrinsic power dissipations from 3% of the Gaussian noise are very high. The frequency bandwidth is wide but becomes narrow at 3% of Gaussian noise (Figure 1.9). The frequency at resonance decreases as the characteristic time increases (Tables 1 to 8). Models of dielectric permittivity in nonlinear dynamics are good interpretive models that can fit the experimental data of solutions of deoxy-hemoglobin S.

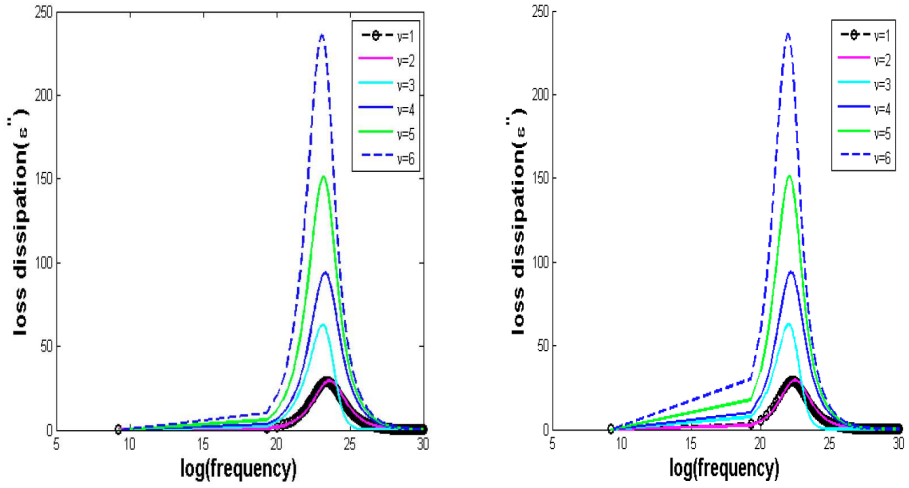


**Figure 1.9.** Power dissipation of the solution 1 by varying the degree of Gaussian noise for times $\tau = 3.334 * 10^{-11}$s (a) and $10^{-10}$s (b).

The peculiarity of the theoretical nonlinear model is that the maximum value of the real permittivity varies and the energy loss is very high at resonance when the degree of Gaussian noise reaches 3% (Table 9).

**Table 9.** Values of the maximum permittivity

| | For $\nu = 1$ | For $\nu = 2$ | For $\nu = 3$ |
|---|---|---|---|
| Solution 1 | 114 | 114 | 162.6534 |
| Solution 2 | 104 | 104 | 144.3288 |
| Solution 3 | 99 | 99 | 136.6001 |
| Solution 4 | 92 | 92 | 128.7161 |

### 3.3. Discussion

We have specified the nature of dehydration in molecular terms. This is because, when the frequency of the erythrocyte solution is less than $\omega = 10^4$ Hz, the red blood cells are in the normal state. During the first phase of the deformation process called the *retardation phase*, the

deformation of red blood cells causes energy loss exponentially when the frequency is greater than $\omega = 10^8$ Hz. The erythrocytes are deformed and their number increases up to the critical frequency $\omega_0$ called the *resonance frequency*, the value of which depends on the relaxation time (Tables 1 to 8). Hematocrit levels are high, red blood cells are difficult to flow, which significantly decreases the uptake and transport of respiratory gases in the blood. On the other hand, subjects suffering from dehydration of the red blood cells develop chronic hemolytic anemia. At the end of the second phase of the kinetic deformation process called the *relaxation phase*, the stresses decrease and the energy loss drops exponentially up to the frequency $\omega = 10^{14}$ Hz. The numerical models presented above clearly describe the phenomenon. Blood being a non-Newtonian fluid whose permittivity decreases when the frequency increases, our results of models in nonlinear dynamics are in excellent agreement with this theory. The hematocrit levels of the erythrocyte solutions studied are high (Tables 1 to 8). Therefore, our theoretical models are suitable for fitting the experimental data of red blood cells to verify the absence of blood abnormalities and diagnose the abnormalities due to dehydration of composite membranes in order to extract information on relaxation and find drugs of synthetic or natural to limit the deformation of composite membranes.

## 4. Conclusion

We have demonstrated the nonlinear effects due to the presence of Gaussian white noise on the example of deoxy-hemoglobin S. The aggregation kinetics of deoxy-hemoglobin S is well interpreted by developing the dielectric permittivity as a function of the relaxation frequency. This development also predicts that the determined hematocrit levels explain very well chronic hemolytic anemia, which may be caused by dehydration. Our study suggests that, our models of dielectric permittivity in nonlinear dynamics are good interpretive models that can fit the experimental data of solutions of deoxy-hemoglobin S.

## References

[1] J. L. Dejardin and L. Olatunji, Mathematical model of deoxyhemoglobin S aggregation kinetics, Journal de Biophysique et de Biomécanique 9(2) (1985), 7579.

[2] J. W. Harris and H. B. Bensusan, The kinetics of solution-gel transformation of deoxy-hemoglobin S by continuous monitoring of viscosity, J. Lab. Clint. Med. 86 (1980), 564.

[3] J. Hofrichter, P. D. Ross and W. A. Easton, Kinetics and mechanism of deoxyhemoglobin S Gelation: a new approach to understanding sickles cell disease, Proc. Natl. Acad. Sci. USA 71 (1974), 4864. http://dx.doi.org/10.1073/pnas.71.12.4864.

[4] D. Quemada, Towards a unified model of elasto-thixotropy of biofluids Biorheology 21 (1984), 423-436.

[5] Batyuk Liliya and Kizilova Nalaliya, Modeling of dielectric permittivity of the erythrocytes membrane as a three-layer model, 2018, pp. 18-37. Doi: http://dx.doi.org/10.30525/978-9934-571-31-2-2.

[6] S. Moussiliou, S. Massou and A. Essoun, Influence of a controlling factor on the unsteady viscosity profile of deoxy-hemoglobin S, Journal of Materials Science Research 1(4) (2012), 79-88. URL: http://dx.doi.org/10.5539/jmsr.v1n4p79.

[7] H. Morgan, T. Sun, D. Holmes, S. Gawad and N. G. Green, Single cell dielectric spectroscopy, J. Phys. D: Appl. Phys. 40 (2007), 6170.

[8] D. Quemada, Rheological modelling of complex fluid, I: The concept of effective volume fraction revisited, The European Physical Journal Applied Physics 1 (1998a), 119-127. http ://dx.doi.org/10.1051/epjap:1998125.

[9] L. O. Olatunji and K. O. Hounsounou, Theoretical study of deoxy-hemoglobin S in simple shear flow, West African J. Biophy. Biomath. 1 (2005), 62.

[10] D. W. Davidson and R. H. Cole, Dielectric relaxation in glycerol, propylene glycol, and n-propanol, J. Chem. Phys. 19 (1951), 1484-1490.

[11] L. O. Olatunji and Mensah, Theoretical study of deoxy-hemoglobin S aggregation in simple shear flow application to steady rheological properties to concentrated dispersions, West African J. Biophy. Biomath. 1 (2005), 88-103.

[12] F. D. Morgan and D. P. Leames, Dielectric relaxation spectra, J. Chem. Phys. 100(1) (1994), 671.

[13] H. Pauly and H. P. Schwan, Dielectric properties and ion mobility in erythrocytes, Biophys. J. 6 (1966), 621-638.